

Nonlinear Compton scattering in a strong rotating electric fieldErez Raicher,^{1,2,*} Shalom Eliezer,^{2,3} and Arie Zigler¹¹*Racah Institute of Physics, Hebrew University, Jerusalem 91904, Israel*²*Department of Applied Physics, Soreq Nuclear Research Center, Yavne 81800, Israel*³*Nuclear Fusion Institute, Polytechnic University of Madrid, 28040 Madrid, Spain*

(Received 3 June 2016; published 6 December 2016)

The nonlinear Compton scattering rate in a rotating electric field is explicitly calculated. For this purpose, an approximate solution to the Klein-Gordon equation in the presence of a rotating electric field is applied. An analytical expression for the emission rate is obtained, as well as a simplified approximation adequate for implementation in kinetic codes. The spectrum is numerically calculated for present-day optical and x-ray laser parameters. The results are compared to the standard Volkov-Ritus rate for a particle in a plane wave, which is commonly assumed to be valid for a rotating electric field under certain conditions. Substantial deviations between the two models, in both the radiated power and the spectral shape, are demonstrated. First, the typical number of photons participating in the scattering process is much smaller compared to the Volkov-Ritus rate, resulting in up to an order of magnitude lower emitted power. Furthermore, our model predicts a discrete harmonic spectrum for electrons with low asymptotic momentum compared to the field amplitude. This discrete structure is a clear imprint of the electric field frequency, as opposed to the Volkov-Ritus rate, which reduces to the constant crossed field rate for the physical conditions under consideration. Our model predictions can be tested with present-day laser facilities.

DOI: [10.1103/PhysRevA.94.062105](https://doi.org/10.1103/PhysRevA.94.062105)**I. INTRODUCTION**

The interaction of electromagnetic (EM) fields with matter is one of the most fundamental problems in physics. The conventional way to introduce the interaction with the photon into the matter equation of motion is by perturbation theory. For this approach to be adequate, the interaction term should be small with respect to the other terms in the Lagrangian. However, if the amplitude of the EM field under consideration exceeds a certain value, a different framework must be adopted. In order to quantitatively characterize the transition to the strong-field regime (where the standard perturbation theory fails), the nonlinearity parameter is introduced

$$\xi \equiv \frac{ea}{m}. \quad (1)$$

Natural units are used ($\hbar = c = 1$), e and m are the electron charge and mass, respectively, and $a \equiv \sqrt{-A_\mu A^\mu}$ is the amplitude of the vector potential A_μ . The intuitive interpretation of ξ , which is the reciprocal of the known Keldysh parameter [1,2], is the typical number of photons participating in the scattering process of the particle and the EM wave. As a result, if $\xi \gg 1$, i.e., in the strong-field regime, it involves many photons absorption. In the opposite case ($\xi < 1$), known as the perturbative regime, a nonlinear process is possible, but the rate W decreases sharply with n (the number of participating photons), namely, $W^{(n)} \propto \xi^{2n}$. In practical units the nonlinearity parameter is given by $\xi = 7.5\sqrt{I[10^{20} \text{ W/cm}^2]}/\omega[\text{eV}]$, where I and ω are the laser intensity and frequency, respectively.

The failure of the standard perturbation technique in the strong-field regime calls for a nonperturbative formalism. The essence of the nonperturbative approach (also known

as the strong-field approximation) is that instead of treating the laser background perturbatively, we include it in the free Lagrangian [3]. Therefore, nonperturbative calculations of quantum electrodynamics (QED) processes in the presence of a laser field (laser assisted) are carried out by replacing the free-electron wave function with the Volkov wave function [4,5]. This wave function is a solution to the quantum equation of motion of a particle interacting with a classical EM plane-wave traveling in vacuum. Employing the above formalism, the properties of QED in the nonperturbative regime were thoroughly investigated both in the 1960s [2,6–11] and in recent years [12–16]. In particular, much attention has been focused on the influence of the temporal and spatial structure of the laser pulse on the strong-field QED processes [17–21]. It should be mentioned that an alternative, fully quantum approach is also feasible [22,23]. Nevertheless, provided the laser pulse depletion due to a single QED process is negligible and the number of photons in the laser quantum mode is much higher than 1, the fully quantum approach reduces to the strong-field one [24]. Since both assumptions are satisfied to an excellent degree in the context of strong laser fields, the strong-field approximation is sufficient.

The experimental exploration of the strong-field regime became feasible due to the invention of the chirped-pulse amplification technique 30 years ago [25]. Since then, the laser intensity has increased eight orders of magnitude to the current record [26] of 10^{22} W/cm^2 at infrared wavelength ($\omega = 1.6 \text{ eV}$), corresponding to $\xi = 50$. Several laser infrastructures with an expected intensity of 10^{24} – 10^{25} W/cm^2 are under construction worldwide, including the three facilities of the ELI project [27]. Several others are in the planning phase, such as the XCELS [28] in Russia, HiPER [29] in the UK, and GEKKO EXA [30] in Japan.

Concurrently, a breakthrough in free-electron laser physics during the 1980s made it possible to achieve intense coherent x-ray light. Nowadays, there are several operating x-ray

*erez.raicher@mail.huji.ac.il

free-electron laser (XFEL) facilities (e.g., LCLS in Stanford [31], SACLA in Japan [32], and FLASH in Hamburg [33]) and one under construction (XFEL in Hamburg [34]). The maximum intensity produced in these facilities lies in the range 10^{20} – 10^{21} W/cm², corresponding to $\xi \approx 2 \times 10^{-3}$.

The experimental availability of such intense field sources creates exciting opportunities in many research fields related to strong-field physics [35,36], such as attosecond spectroscopy [37], relativistic nonlinear optics and relativistic high-order harmonic generation [38,39], ultrastrong laser-plasma interaction and particle acceleration [40,41], laboratory astrophysics [42], laser-assisted QED processes [43,44], Schwinger pair production [45], and exotic nuclear physics [46].

This work is devoted to one of the most significant laser-assisted QED processes, nonlinear Compton scattering. Unlike the standard Compton process, where a photon scatters off an electron, nonlinear Compton scattering describes the coherent interaction of many photons with an electron. The outgoing particles are the electron and a single energetic photon. This scattering is of particular significance for several reasons. First, it may be used to create γ sources in the interaction of ultraintense lasers with an energetic electrons beam. Second, it is one of the main processes responsible for the electron radiation losses in the interaction of ultraintense lasers with plasma. In particular, the interplay between this process and the Breit-Wheeler process, involving a hard photon interacting with many laser photons to create an electron-positron pair, may result in a mechanism called QED cascade in the following way. The hard photon emitted during nonlinear Compton scattering decays into an electron-positron pair through the Breit-Wheeler scattering. The newly created particles also radiate hard photons through nonlinear Compton scattering, leading to the emergence of an avalanche. These QED cascades have attracted increasing scientific attention [47–57] for both fundamental and practical reasons. Practically, spontaneous cascades may drain energy from the laser pulse and thus limit the utmost attainable intensity [50]. From a fundamental point of view, the cascades are of interest as they result in a QED plasma (namely, electrons, positrons, and γ photons) resembling many astrophysical scenarios [48].

The most favorable configuration to achieve the QED cascade is a rotating electric field [51]. It may be realized in the vicinity of the antinodes of a standing wave formed by two counterpropagating laser beams. The standard kinetic modeling consists of a particle-in-cell (PIC) code to describe the plasma motion combined with a Monte Carlo QED module to account for the strong-field QED emission processes listed above. The QED rates are those obtained by the Volkov wave function, though the EM field configuration is different from the one used in the Volkov derivation.

The justification to this approximation was formulated by Nikishov and co-workers [2,11] (see also the comprehensive review [44]). Their derivation is based on the Volkov solution and from now on will be referred to as the Volkov-Ritus solution. The explanation of their argument requires the introduction of the four dimensionless quantities on which the quantum rate depends. The first is the field strength ξ introduced above. The second is the normalized acceleration experienced by the particle in its rest frame. It is known as the

quantum parameter and takes the form [44]

$$\chi \equiv \frac{e}{m^3} \sqrt{-(F^{\mu\nu} \Pi_\nu)^2}, \quad (2)$$

where Π_ν is the eigenvalue of the kinetic momentum operator $-i\partial_\mu - eA_\mu$ and the EM field strength tensor is given by

$$F_{\mu\nu} = \partial_\mu A_\nu - \partial_\nu A_\mu. \quad (3)$$

The classical regime, i.e., the nonlinear Thomson scattering, corresponds to $\chi \ll 1$. The next-generation lasers are expected to enter the quantum regime $\chi \approx 1$. Two additional quantities are the EM field invariants

$$\mathcal{F} \equiv \frac{e^2 F_{\mu\nu} F^{\mu\nu}}{4m^4}, \quad \mathcal{G} \equiv \frac{\epsilon_{\alpha\beta\mu\nu} e^2 F^{\alpha\beta} F^{\mu\nu}}{4m^4}. \quad (4)$$

The symbol $\epsilon_{\alpha\beta\mu\nu}$ stands for the Levi-Civita tensor. Ritus and Nikishov argued that as long as the conditions

$$\mathcal{F}, \mathcal{G} \ll \chi^2, \quad \mathcal{F}, \mathcal{G} \ll 1, \quad \xi \gg 1 \quad (5)$$

hold, the rate is well described by the Volkov-Ritus expression (coinciding under these conditions with the emission in a constant crossed field).

However, it was recently demonstrated by the present authors [58] that the wave function of a particle in a rotating electric field exhibits significant deviation from the Volkov solution even if (5) is satisfied. Consequently, we are motivated to explore the emission rate of an electron in this field configuration, corresponding to our wave function, as compared to the familiar Volkov-Ritus rate. For the sake of simplicity, the investigation was carried out for the scalar case, neglecting the spin effects. These were shown to be of secondary importance for ultraintense laser-particle interaction [59].

The paper is organized as follows. In Sec. II the strong-field Lagrangian is written down and the second quantization is outlined. Section III reviews the analytical solution derived in [58] for a particle in a rotating electric field. Section IV describes the phase-space factor appearing in the nonlinear Compton scattering rate. Section V includes a detailed calculation of the matrix element. In Sec. VI we explicitly show that in the proper conditions our formula recovers the Volkov-Ritus one. Section VII deals with a continuum approximation to our rate, Sec. VIII considers the radiation coherence time interval, and Sec. IX contains the final expression for the emission spectrum. In Sec. X the present rate is evaluated numerically and compared to the Volkov-Ritus expression for physical parameters corresponding to present-days laser facilities. Section XI summarizes the paper.

II. LAGRANGIAN FORMULATION

The final goal of this work is the calculation of the nonlinear Compton scattering rate in a rotating electric field. For this purpose, a Lagrangian formulation of the problem, including second quantization, is required. This framework, known as strong-field QED, was developed for the Volkov problem long ago [3,44] and was recently generalized by the present authors [60] for the case of a rotating electric field. The main results of the generalization are given below.

The Lagrangian of the scalar QED reads

$$\mathcal{L}_{sQED} = \frac{1}{2} \partial_\mu \Phi^* \partial^\mu \Phi - \frac{1}{2} m^2 \Phi^* \Phi - \frac{1}{16\pi} F_{\mu\nu} F^{\mu\nu} + A_\mu (f_1^\mu + A^\mu f_2), \quad (6)$$

where Φ is the scalar field operator. The last term in the Lagrangian, representing the interaction between light and matter, is expressed using the definitions

$$f_1^\mu \equiv \frac{1}{2} i e (\Phi^* \partial^\mu \Phi - \Phi \partial^\mu \Phi^*) \quad (7)$$

and

$$f_2 \equiv \frac{1}{2} e^2 |\Phi|^2. \quad (8)$$

In standard QED, the interaction term in (6) is considered as a perturbation. However, in the presence of a strong field, A_μ acquires a vacuum expectation value and the interaction term should be redefined according to Furry [3],

$$A_\mu = A_\mu^{cl} + A_\mu^Q, \quad A_\mu^{cl} \equiv \langle \Omega | A_\mu | \Omega \rangle, \quad (9)$$

where $|\Omega\rangle$ stands for the vacuum state and will be defined below. We substitute (9) into (6) and group all terms involving both A_μ^Q and f_1^μ, f_2 ,

$$\mathcal{L}_{\text{int}} = 2f_2(A^{cl} \cdot A^Q) + A^Q \cdot f_1 + (A^Q)^2 f_2, \quad (10)$$

where the center dot stands for Lorentz contraction. The remaining terms are included in the free part of the Lagrangian

$$\mathcal{L}_{\text{free}} = \frac{1}{2} \partial_\mu \Phi^* \partial^\mu \Phi - \frac{1}{2} m^2 \Phi^* \Phi - \frac{1}{16\pi} F_{\mu\nu} F^{\mu\nu} + \mathcal{L}_{\text{Furry}}, \quad (11)$$

where

$$\mathcal{L}_{\text{Furry}} = A^{cl} \cdot f_1 + f_2 A^{cl2}. \quad (12)$$

Finally, the full Lagrangian is the sum $\mathcal{L} = \mathcal{L}_{\text{free}} + \mathcal{L}_{\text{int}}$. The free equations of motion corresponding to (11) are

$$[-\partial^2 + e^2 A^{cl2} - 2ieA^{cl} \cdot \partial - m^2] \Phi = 0, \quad (13)$$

$$\partial^2 A_\mu^Q = 0, \quad (14)$$

$$\partial^2 A_\mu^{cl} = 0. \quad (15)$$

The solution of the system, addressed in the next section, enables us to proceed with the second quantization procedure

$$\Phi = \int \frac{d^3 q}{(2\pi)^3 \sqrt{2q_0}} [c_q \phi_A(q) + \text{H.c.}], \quad (16)$$

$$A_\mu^Q = \int \frac{d^3 k'}{(2\pi)^3 \sqrt{2k'_0}} [\epsilon'_\mu a_{k'} e^{-ik' \cdot x} + \text{H.c.}], \quad (17)$$

where ϵ'_μ is the photon polarization vector and $\phi_A(q)$ and $\epsilon'_\mu e^{-ik' \cdot x}$ are the one-particle solution of (13) and (15), respectively. The quasimomentum q_μ is a 4-vector characterizing the wave function ϕ_A and will be defined in the next section. We introduced the creation and annihilation operators, obeying the

commutation relations

$$[a_{k'}^\dagger, a_{k''}] = (2\pi)^3 \delta^3(k'' - k'), \quad (18)$$

$$[c_q^\dagger, c_{q'}] = (2\pi)^3 \delta^3(q - q'). \quad (19)$$

Now let us specify the vacuum state $|\Omega\rangle$ and the corresponding classical field A_μ^{cl} . As was mentioned in the Introduction, a rotating electric field can be realized at the antinodes of a standing wave formed by colliding circularly polarized laser beams. The vector potential corresponding to this configuration is

$$A^{cl,\mu} = \frac{1}{2} a_1^\mu [\cos(k_1 \cdot x) + \cos(k_2 \cdot x)] + \frac{1}{2} a_2^\mu [\sin(k_1 \cdot x) + \sin(k_2 \cdot x)], \quad (20)$$

where the wave vectors are $k_1^\mu = (\omega, \mathbf{k})$ and $k_2^\mu = (\omega, -\mathbf{k})$ and satisfy the vacuum dispersion relation $k_1^2 = k_2^2 = 0$. The polarization vectors are given by

$$a_1^\mu = a(k \cdot x) \hat{e}_1^\mu, \quad a_2^\mu = a(k \cdot x) \hat{e}_2^\mu, \quad (21)$$

where $a(k \cdot x)$ is a slowly varying amplitude vanishing at $k \cdot x \rightarrow \pm\infty$. However, in the following this envelope is assumed to be slow enough [$da/d(k \cdot x) \ll 1$, corresponding to a many-cycle pulse] so that a is approximately constant. As a result, the influence of the ponderomotive force as well as finite pulse effects is beyond the scope of our model. The unit vectors read

$$\hat{e}_1^{\text{lab}} = (0, 1, 0, 0), \quad \hat{e}_2^{\text{lab}} = (0, 0, 1, 0), \quad (22)$$

where the superscript *lab* attached to a 4-vector denotes that it is evaluated in the laboratory frame of reference. Notice that A^{cl} given by (20) satisfies, as it should, the relevant equation of motion (15). The ground state corresponding to this field configuration is

$$|\Omega\rangle = |0\rangle |\alpha, k_1; \alpha, k_2\rangle, \quad (23)$$

where $|0\rangle$ is the scalar part of the wave function and $|\alpha, k_1; \alpha, k_2\rangle$ stands for two coherent states with 4-momenta k_1, k_2 , respectively, representing the counterpropagating laser beams.

III. ANALYTICAL SOLUTION

In the previous section, the equation of motion describing the dynamics of the scalar field operator was derived (13). Substituting the ansatz (16) for Φ , one may obtain the equation satisfied by the one-particle wave function ϕ_A ,

$$[-\partial^2 - 2ie(A^{cl} \cdot \partial) + e^2 A^{cl2} - m^2] \phi_A = 0, \quad (24)$$

which is the familiar Klein-Gordon equation in the presence of a classical EM field. Using simple trigonometric manipulations, the laser field (20) takes the form

$$A^{cl,\mu} = \cos(\mathbf{k} \cdot \mathbf{x}) [a_1^\mu \cos(\omega t) + a_2^\mu \sin(\omega t)]. \quad (25)$$

In the vicinity of the antinode, i.e., $\mathbf{k} \cdot \mathbf{x} = 0$, the cosine equals unity up to a second-order correction, i.e., $\cos(\mathbf{k} \cdot \mathbf{x}) \cong 1$. In order to cast Eq. (25) into a Lorentz-invariant form, namely,

$$A^{cl,\mu} = a_1^\mu \cos(k \cdot x) + a_2^\mu \sin(k \cdot x), \quad (26)$$

a wave vector k_μ is introduced. In the laboratory frame it reads $k^{\text{lab}} = (\omega, 0, 0, 0)$. Consequently, it obeys a massivelike dispersion relation

$$k^2 \equiv m_{ph}^2 > 0, \quad (27)$$

where m_{ph} is the effective mass of the rotating electric field photons. As can be inferred from the definition of k , the photon effective mass equals the laser frequency in the laboratory frame, $m_{ph} = \omega$.

The dynamics of Eqs. (24), (26), and (27) were investigated by several authors [61–66]. It was shown that if one assumes a massivelike dispersion relation for the EM field then the Klein-Gordon equation reduces to the Mathieu ordinary differential equation. In the following we will employ an approximate solution to the Mathieu equation, recently published by the present authors [58]. This solution was also generalized to a standing wave [67] and compared to other approaches such as the WKB or perturbative method in [68].

The approximate wave function $\phi_A(q)$ solving (24) takes the form [58]

$$\begin{aligned} \phi_A(q) = \exp \left[-iq \cdot x - i \frac{e(a_1 \cdot q)}{k \cdot q} \sin(k \cdot x) \right. \\ \left. + i \frac{e(a_2 \cdot q)}{k \cdot q} \cos(k \cdot x) \right]. \end{aligned} \quad (28)$$

The quasimomentum is defined as

$$q_\mu \equiv p_\mu - \nu k_\mu, \quad (29)$$

where p_μ is the asymptotic momentum (the momentum in the absence of the EM wave) and ν is the characteristic exponential given by

$$\nu = \frac{k \cdot p}{m_{ph}^2} \left[1 - \sqrt{1 + \left(\frac{eam_{ph}}{k \cdot p} \right)^2} \right]. \quad (30)$$

In the limit $m_{ph} \rightarrow 0$, the characteristic exponential reduces to the Volkov expression, namely, $\nu \rightarrow \nu^V = -(ea)^2/2(k \cdot p)$. As a result, the Volkov solution is recovered.

The underlying assumption behind this approximated solution is

$$\delta \equiv \frac{eam_{ph}^2 |p \cdot (\hat{e}_1 + i\hat{e}_2)|}{(k \cdot q)^2} \ll 1. \quad (31)$$

Equivalently, in the laboratory frame, it takes the form

$$\delta \equiv \frac{eap_\perp^{\text{lab}}}{(ea)^2 + (p_0^{\text{lab}})^2} \ll 1, \quad (32)$$

where $p_\perp \equiv \sqrt{p_x^2 + p_y^2}$ is the perpendicular asymptotic momentum. The physical meaning of this condition is that our approximation is valid unless the perpendicular asymptotic momentum is comparable to both the field amplitude and the asymptotic energy (i.e., $p_\perp^{\text{lab}} \approx p_0^{\text{lab}}$ and $p_\perp^{\text{lab}} \approx ea$).

Let us calculate three significant quantities associated with the wave function. The first is the dressed electron effective mass, frequently encountered in the following sections. Using the definition $m_* \equiv \sqrt{q^2}$ and (29), one obtains

$$m_* = m\sqrt{1 + \xi^2}, \quad (33)$$

which is identical to the expression corresponding to the Volkov wave function [44]. The second quantity is the eigenvalue Π_μ of the kinetic momentum operator, satisfying

$$(-i\partial_\mu - eA_\mu)\phi_A = \Pi_\mu\phi_A. \quad (34)$$

Evaluating the left-hand side of the above equation, one finds

$$\Pi_\mu = p_\mu - eA_\mu - \nu k_\mu, \quad (35)$$

which is nothing but the classical momentum of a particle in a rotating electric field. The third quantity to be calculated is the quantum parameter χ , obtained by substituting (35) into (2),

$$\chi = \frac{ea(k \cdot q)}{m^3} \sqrt{1 - \frac{m_{ph}^2(A^{cl'} \cdot p)^2}{(ea)^2(k \cdot q)^2}}, \quad (36)$$

where $A^{cl'}$ denotes the first derivative of A^{cl} with respect to $(k \cdot x)$. Notice that χ is time dependent (through $A^{cl'}$) unless the asymptotic momentum satisfies $A^{cl'} \cdot p = 0$.

IV. SCATTERING PHASE SPACE

In the following, the nonlinear Compton scattering rate corresponding to our present solution is obtained. According to the standard formulation, we start with the transition amplitude between the initial and final states and relate it to the interaction Lagrangian. Afterward, the rate is written as a matrix element integrated over the available phase space of the outgoing particles. This section mainly deals with the particulars of the phase-space integration, while the matrix element calculation is addressed in the next one.

The transition amplitude iT between the initial and final states reads

$$iT = \langle q', k' | (\mathcal{S} - 1) | q \rangle, \quad (37)$$

where the canonical normalization is used for the one particle states, i.e., $|q\rangle \equiv \sqrt{2q_0} c_q^\dagger(q) |\Omega\rangle$. The scattering matrix in the interaction picture is given by

$$\mathcal{S} = \mathcal{T} \exp \left(i \int d^4x \mathcal{L}_{\text{int}} \right), \quad (38)$$

where \mathcal{T} is the time ordering operator and \mathcal{L}_{int} was given in (10). The nonlinear Compton scattering originates in the first-order term in the Taylor expansion of \mathcal{S} . Hence,

$$iT = \langle q', k' | \int d^4x \mathcal{L}_{\text{int}} | q \rangle. \quad (39)$$

Omitting the term in (10) involving $(A_\mu^Q)^2$ (since it does not contribute to this scattering) and writing explicitly f_1^μ, f_2 , we obtain

$$\mathcal{L}_{\text{int}} = eA^{Q;\mu} [\Phi^*(i\partial_\mu + eA_\mu^{cl})\Phi - \Phi(i\partial_\mu - eA_\mu^{cl})\Phi^*]. \quad (40)$$

Substituting (16), (17), and (40) into (39), the transition amplitude takes the form

$$\begin{aligned} iT = ie \int dx^4 (\epsilon'_\mu)^* e^{ik' \cdot x} [\phi_A^*(q') (i\partial^\mu + eA_\mu^{cl}) \phi_A(q) \\ - \phi_A(q) (i\partial^\mu - eA_\mu^{cl}) \phi_A^*(q')]. \end{aligned} \quad (41)$$

As explicitly shown later on, the integration over d^4x results in an infinite sum of energy-momentum-conservation delta

functions

$$iT = i \sum_s \mathcal{M}_s (2\pi)^4 \delta^4(q + sk - k' - q'), \quad (42)$$

where \mathcal{M}_s is the matrix element and s is the number of laser photons absorbed in the process. Let us consider a process with a given s . The corresponding energy-momentum conservation reads

$$sk + q = q' + k'. \quad (43)$$

It is favorable to hold our discussion in the center-of-mass frame. Let us write down the incoming 4-momenta explicitly

$$sk = (\sqrt{p_{\text{in}}^2 + s^2 m_{ph}^2}, 0, 0, p_{\text{in}}), \quad (44)$$

$$q = (\sqrt{p_{\text{in}}^2 + m_*^2}, 0, 0, -p_{\text{in}}), \quad (45)$$

where p_{in} is the momentum of each of the incoming particles in the center-of-mass frame. The 4-momenta of the outgoing particles are

$$q' = p_{\text{out}} \left(\sqrt{1 + \left[\frac{m_*}{p_{\text{out}}} \right]^2}, \sin \theta \cos \varphi, \sin \theta \sin \varphi, \cos \theta \right), \quad (46)$$

$$k' = p_{\text{out}} (1, -\sin \theta \cos \varphi, -\sin \theta \sin \varphi, -\cos \theta), \quad (47)$$

where θ and φ are the scattering angles and p_{out} is the momentum of the outgoing particles in the center-of-mass frame. The center-of-mass energy is given by

$$E_s^2 = (sk + q)^2 = s^2 m_{ph}^2 + m_*^2 + 2sk \cdot q. \quad (48)$$

The initial center-of-mass momentum is related to E_s by

$$E_s = sk_0 + q_0 = \sqrt{s^2 m_{ph}^2 + p_{\text{in}}^2} + \sqrt{m_*^2 + p_{\text{in}}^2}. \quad (49)$$

The solution of equation (49) yields

$$p_{\text{in}} = \frac{s(k \cdot q)}{E_s} \sqrt{1 - \left(\frac{m_* m_{ph}}{k \cdot q} \right)^2}. \quad (50)$$

The final center-of-mass momentum is related to E_s by

$$E_s = p_{\text{out}} + \sqrt{m_*^2 + p_{\text{out}}^2}. \quad (51)$$

Hence we have

$$p_{\text{out}} = \frac{E_s^2 - m_*^2}{2E_s} = \frac{s^2 m_{ph}^2 + 2sk \cdot q}{2E_s}. \quad (52)$$

For vanishing m_{ph} Eqs. (49) and (51) take exactly the same form. Therefore, Eqs. (50) and (52) become identical ($p_{\text{in}} = p_{\text{out}}$), as expected.

In order to obtain the total emission rate for a hard photon by the electron, the phase-space integration should be performed. The rate W is related to the transition amplitude by [5]

$$W = \frac{1}{2q_0} \int \frac{d^3 q'}{(2\pi)^3 2q'_0} \frac{d^3 k'}{(2\pi)^3 2k'_0} |T|^2. \quad (53)$$

Notice that the integration result is Lorentz invariant and the only frame-dependent term is the coefficient $1/2q_0$ multiplying

the integral. The δ function appearing in the expression for $|T|^2$ contains four constraints on the possible final states. Therefore, the summation over the phase space reduces to a two-dimensional integral [69]

$$\delta^4(sk + q - q' - k') \frac{d^3 q' d^3 k'}{q'_0 k'_0} \rightarrow \frac{p_{\text{out}} d(\cos \theta) d\varphi}{E_s}. \quad (54)$$

Since each s has a unique center-of-mass frame, different s corresponds to different θ . As a result, we would like to replace $\cos \theta$ in (54) by a more convenient variable. For this purpose, a Lorentz-invariant parameter is introduced

$$u \equiv \frac{k \cdot k'}{k \cdot q'}. \quad (55)$$

This variable is also an indicator of the classical or quantum nature of the scattering [44]. Since $u \ll 1$ implies a negligible momentum of the outgoing photon, it corresponds to the classical limit. On the other hand, for $u \approx 1$ the quantum mechanics dominates the process. In the strong-field regime ($\xi \gg 1$) one may show that $u \approx 1$ corresponds to $\chi \approx 1$. One may show that θ is related to u by (see Appendix A)

$$\cos \theta = \eta_s \left(\kappa_s - \frac{\kappa_s + 1}{1 + u} \right), \quad (56)$$

with

$$\kappa_s \equiv \frac{E_s^2 + m_*^2}{E_s^2 - m_*^2} \quad (57)$$

and

$$\eta_s \equiv \frac{sk_0}{p_{\text{in}}}. \quad (58)$$

Notice that in the Volkov limit (i.e., $m_{ph} \rightarrow 0$) we have $\eta_s = 1$ by definition, due to the vacuum dispersion of the laser photons. In order to obtain η_s in terms of the initial quantities, Eq. (50) and the relation $k_0 = \sqrt{m_{ph}^2 + (p_{\text{in}}/s)^2}$ are employed:

$$\eta_s = \sqrt{\frac{(k \cdot q)^2 + 2s(k \cdot q)m_{ph}^2 + s^2 m_{ph}^4}{(k \cdot q)^2 - (m_{ph} m_*)^2}}. \quad (59)$$

In the laboratory frame, $k \cdot q = m_{ph} q_0^{\text{lab}}$. As a result, Eq. (59) simplifies to

$$\eta_s = \frac{q_0^{\text{lab}} + sm_{ph}}{\sqrt{(q_0^{\text{lab}})^2 - m_*^2}}. \quad (60)$$

The limiting values of u , corresponding to $\cos \theta = \pm 1$, are

$$u_{s,\text{min}} = \frac{\eta_s - 1}{\eta_s \kappa_s + 1}, \quad u_{s,\text{max}} = \frac{\eta_s + 1}{\eta_s \kappa_s - 1}. \quad (61)$$

For vanishing m_{ph} the well-known Volkov-Ritus expression is recovered, namely, $u_{s,\text{min}}^V = 0$ and

$$u_{s,\text{max}}^V = \left(\frac{E_s}{m_*} \right)^2 - 1. \quad (62)$$

Finally, the phase-space factor (54) may be written as

$$\delta^4(sk + q - q' - k') \frac{d^3 q' d^3 k'}{q'_0 k'_0} \rightarrow \frac{\eta_s du d\varphi}{(1 + u)^2}. \quad (63)$$

Substituting (63) into (53) and summing over the polarization of the outgoing photon, the rate is obtained

$$\frac{dW}{dud\varphi} = \sum_s \frac{dW_s}{dud\varphi}, \quad (64)$$

$$\frac{dW_s}{dud\varphi} = \frac{\eta_s}{32\pi^2 q_0(1+u)^2} \times \frac{1}{2} \sum_{\epsilon'} |\mathcal{M}_{s,\epsilon'}|^2. \quad (65)$$

Notice that the matrix element is averaged over the polarization ϵ' of the emitted photon. The total rate is obtained by integrating (64) with respect to u, φ in the range $0 < \varphi < 2\pi$ and $u_{\min} < u < u_{\max}$. In order to return to the cgs unit system the simple transformations $m \rightarrow mc^2$, $m_{ph} \rightarrow m_{ph}c^2$, and $q \rightarrow \hbar q$ are carried out.

V. MATRIX ELEMENT CALCULATION

In the preceding section, a relation between the transition amplitude and the particle wave function was established (41). In the following, it is further evaluated and expressed in terms of the initial quantities. Substituting the analytical wave functions (28) into (41), we arrive at

$$iT = ie \int d^4x (\epsilon'^{\mu})^* e^{iQ} \left[q_\mu + q'_\mu + \left(\frac{e(q \cdot A^{cl})}{(k \cdot q)} + \frac{e(q' \cdot A^{cl})}{(k \cdot q')} \right) k_\mu - 2eA_\mu^{cl} \right], \quad (66)$$

where the exponent argument is

$$Q \equiv (q' - q + k') \cdot x + \alpha_1 \sin(k \cdot x) - \alpha_2 \cos(k \cdot x) \quad (67)$$

and the following quantities are introduced:

$$\alpha_i \equiv \frac{e(a_i \cdot q)}{(k \cdot q)} - \frac{e(a_i \cdot q')}{(k \cdot q')}, \quad i = 1, 2. \quad (68)$$

It proves useful to rewrite the following expression, appearing in the exponent argument:

$$\alpha_1 \sin(k \cdot x) - \alpha_2 \cos(k \cdot x) = z \sin[(k \cdot x) - \phi_0], \quad (69)$$

with the definitions

$$z \equiv \sqrt{\alpha_1^2 + \alpha_2^2} \quad (70)$$

and

$$\phi_0 \equiv \tan^{-1}(\alpha_1/\alpha_2). \quad (71)$$

As shown below, the phase ϕ_0 does not appear in the final expression and therefore bears no physical meaning.

In order to carry out the integration, we take advantage of the identity

$$[1, \cos(k \cdot x), \sin(k \cdot x)] e^{iz \sin[(k \cdot x) - \phi_0]} = \sum_s (B, B_1, B_2) e^{is(k \cdot x)}, \quad (72)$$

where

$$B \equiv J_s(z) e^{is\phi_0}, \quad (73)$$

$$B_1 \equiv \left(\frac{s}{z} J_s(z) \cos \phi_0 + i J'_s(z) \sin \phi_0 \right) e^{is\phi_0}, \quad (74)$$

$$B_2 \equiv \left(\frac{s}{z} J_s(z) \sin \phi_0 - i J'_s(z) \cos \phi_0 \right) e^{is\phi_0}, \quad (75)$$

and $J_s(z)$ is the Bessel function. In terms of B, B_1, B_2 , the integration of (66) yields

$$iT = i \sum_s \mathcal{M}_s (2\pi)^4 \delta^4(q + sk - k' - q'), \quad (76)$$

where the matrix element takes the form

$$i\mathcal{M}_s = ie\epsilon'_\mu \left[(q^\mu + q'^\mu)B - 2eB_1 a_1^\mu - 2eB_2 a_2^\mu + e(a_1 + a_2) \cdot \left(\frac{q}{k \cdot q} + \frac{q'}{k \cdot q'} \right) k^\mu \right] \quad (77)$$

and the expression for A_μ^{cl} (26) was used. The next step is to sum over the emitted photon polarization. For this purpose, we introduce the quantity \mathcal{M}_μ , defined by

$$\mathcal{M} \equiv \mathcal{M}_\mu \epsilon'^{\mu}. \quad (78)$$

Due to the dispersion of the emitted photon, namely, $k'^2 = 0$, one can apply the Ward identity [69] and therefore the summation over the outgoing photon polarization is simplified to

$$\sum_{\epsilon'} |\mathcal{M}|^2 = -g^{\mu\nu} \mathcal{M}_\mu \mathcal{M}_\nu^*, \quad (79)$$

where $g^{\mu\nu} \equiv \text{diag}(1, -1, -1, -1)$ is the Minkowski metric. Substituting (77) and (78) into (79), the final expression is obtained (see Appendix B for details)

$$\frac{1}{2} \sum_{\epsilon'} |\mathcal{M}_{s,\epsilon'}|^2 = -2e^2 J_s^2(z) \left(2m_*^2 + \frac{u-3}{2(u+1)} s^2 m_{ph}^2 \right) + 4e^4 a^2 \left(\frac{s^2}{z^2} J_s^2(z) + J_s'^2(z) \right). \quad (80)$$

At the moment, the variable z (necessary to calculate the matrix element) depends upon the unknown quantities

$$(k \cdot q'), (q' \cdot a_1), (q' \cdot a_2). \quad (81)$$

Let us express (81) in terms of the Lorentz invariants

$$s, (k \cdot q), (q \cdot a_1), (q \cdot a_2), u, \varphi. \quad (82)$$

We start with $k \cdot q'$. Using (A1) from Appendix A, we simply get

$$k \cdot q' = \frac{sm_{ph}^2 + k \cdot q}{u+1}. \quad (83)$$

As for $(q' \cdot a_1), (q' \cdot a_2)$, a parametrization of the vector potential in the center-of-mass frame is required. We assume, without loss of generality, that the momentum of the incoming particle lies (in the laboratory frame) in the x - z plane. Hence, in the center-of-mass frame a_2 remains unchanged,

$$a_2 = a(0, 0, 1, 0), \quad (84)$$

and by definition $a_2 \cdot q = 0$. In Appendix C, an expression for a_1 in the center-of-mass frame is derived

$$a_1 = a[R_0, \sqrt{1 - R_0^2(\eta_s^2 - 1)^2}, 0, R_0\eta_s], \quad (85)$$

where

$$R_0 = \frac{q \cdot a_1}{aE_s}. \quad (86)$$

Employing (84), (85), and (46), the evaluation of $(q' \cdot a_1), (q' \cdot a_2)$ is straightforward

$$a_2 \cdot q' = -ap_{\text{out}} \sin \theta \sin \varphi \quad (87)$$

and

$$a_1 \cdot q' = ap_{\text{out}} \left[R_0 \sqrt{1 + \left(\frac{m_*}{p_{\text{out}}} \right)^2} + R_0 \eta_s \cos \theta - \sin \theta \cos \varphi \sqrt{1 - R_0^2(\eta_s^2 - 1)} \right]. \quad (88)$$

Plugging the above equations into (68), we obtain α_1, α_2 :

$$\alpha_2 = \frac{eap_{\text{out}} \sin \theta \sin \varphi (1 + u)}{k \cdot q + sm_{ph}^2} \quad (89)$$

and

$$\alpha_1 = \frac{e(a_1 \cdot q)}{k \cdot q} - \frac{eap_{\text{out}}(u + 1)}{k \cdot q + sm_{ph}^2} \left[R_0 \sqrt{1 + \left(\frac{m_*}{p_{\text{out}}} \right)^2} + R_0 \eta_s \cos \theta - \sin \theta \cos \varphi \sqrt{1 - R_0^2(\eta_s^2 - 1)} \right]. \quad (90)$$

To sum up, the final expression for the matrix element is (80), where z is calculated using (70), (89), and (90).

In the above derivation, z depends on both u and φ , as opposed to the Volkov-Ritus case (where it depends upon u only). Notice, however, that under the condition $q \cdot a_1 = 0$, we have $R_0 = 0$ and the dependence on φ vanishes. The expression for z simplifies to

$$z = \frac{eap_{\text{out}}}{sm_{ph}^2 + k \cdot q} \sin \theta (1 + u). \quad (91)$$

Employing (56), the angle θ may be written in terms of u :

$$\sin \theta (1 + u) = \sqrt{\bar{A}_s u^2 + \bar{B}_s u + \bar{C}_s} \quad (92)$$

with

$$\bar{A}_s \equiv 1 - \kappa_s^2 \eta_s^2, \quad \bar{B}_s \equiv 2(\kappa_s \eta_s^2 + 1), \quad \bar{C}_s \equiv 1 - \eta_s^2. \quad (93)$$

By equating the derivative of (92) with zero, one can readily obtain the u value corresponding to the maximum of this function

$$u_s^m = \frac{\eta_s^2 \kappa_s + 1}{\eta_s^4 \kappa_s^2 - 1}. \quad (94)$$

By definition, the contribution of a given harmonic s is centered around $u = u_s^m$. The substitution of (94) into (92) yields the maximal value of this function

$$\bar{D}_s \equiv \sin \theta (1 + u)|_{\text{max}} = \frac{\eta_s(\eta_s \kappa_s + 1)}{\sqrt{\eta_s^4 \kappa_s^2 - 1}}. \quad (95)$$

VI. VOLKOV-RITUS LIMIT

The matrix element calculation being completed, a benchmark with an established result is valuable. For vanishing m_{ph} , the quantum problem is identical to the one solved by Volkov. Consequently, the results obtained in the previous section should recover the familiar Volkov-Ritus formulas [44]. In the following, this limit is explicitly worked out.

We start with expression for the matrix element derived in the previous section (80). For $m_{ph} = 0$, the second term vanishes and the familiar Volkov-Ritus expression for scalars [44] is reproduced

$$\frac{1}{2} \sum_{\epsilon'} |\mathcal{M}_{s,\epsilon'}|_V^2 = -4e^2 J_s^2(z) m_*^2 + 4e^4 a^2 \left(\frac{s^2}{z^2} J_s^2(z) + J_s'^2(z) \right). \quad (96)$$

One can observe that the Volkov-Ritus matrix element (96) is not very different from that obtained earlier (80). The major difference, however, lies in the dependence of z on the particle's incoming momentum, as shown below.

Let us find z in the Volkov-Ritus limit. For a vanishing m_{ph} we have $\eta_s = 1$, as can be seen from (58). Therefore, the formula (90) for α_1 simplifies to

$$\alpha_1 = \frac{eap_{\text{out}} \sin \theta \cos \varphi}{k \cdot q} + \frac{e(a_1 \cdot q)}{k \cdot q} \left[1 - \frac{(u + 1)p_{\text{out}}}{E_s} \times \sqrt{1 + \left(\frac{m_*}{p_{\text{out}}} \right)^2} + \frac{(u + 1)p_{\text{out}} \cos \theta}{E_s} \right]. \quad (97)$$

Using (A7) from Appendix A, the last term is rewritten

$$\frac{(u + 1)p_{\text{out}} \cos \theta}{E_s} = \frac{(u + 1)}{E_s} \left(q'_0 - \frac{E_s}{1 + u} \right). \quad (98)$$

Plugging (98) into (97), one can observe that the term in square brackets in (97) is identically zero. Thus, z may be cast in the form

$$z = \frac{eap_{\text{out}}}{k \cdot q} \sin \theta (1 + u). \quad (99)$$

From $\eta_s = 1$ we deduce that $\bar{C}_s = 0$ and therefore (92) simplifies to

$$\sin \theta (1 + u) = \frac{2E_s m_*}{E_s^2 - m_*^2} \sqrt{u(u_{s,\text{max}}^V - u)}, \quad (100)$$

where $u_{s,\text{max}}^V$ was defined in (62). The substitution of (52) and (100) into (99) yields

$$z = \frac{eam_*}{k \cdot q} \sqrt{u(u_{s,\text{max}}^V - u)}. \quad (101)$$

In the absence of m_{ph} , Eq. (36) implies that $k \cdot q$ is simply related to the quantum parameter, namely, $\chi = \frac{ea(k \cdot q)}{m^3}$. Consequently, the familiar Volkov-Ritus expression is recovered

$$z = \frac{\xi^2 \sqrt{1 + \xi^2}}{\chi} \sqrt{u(u_{s,\text{max}}^V - u)}, \quad (102)$$

where (1) and (33) were used as well.

VII. CONTINUUM APPROXIMATION

As explicitly demonstrated in Sec. V, the emission spectrum is composed of $s \rightarrow \infty$ harmonics. As a matter of fact, the number of harmonics with non-negligible probability depends upon the nonlinearity parameter ξ . In the Volkov-Ritus rate, for instance, the spectrum peak corresponds to $s \propto \xi^3$ in the strong-field regime, $\xi \gg 1$. If the emission spectrum consists of a large number of overlapping harmonics, it becomes a continuous function. In the following, we seek the continuous limit of the rate obtained above (64), (65), and (80). For the sake of simplicity, the discussion is limited to the case of $q \cdot a_1 = 0$, where the φ dependence vanishes and the expression for z is simpler (91).

The essence of this approximation is the replacement of the sum over the harmonics by an integral, i.e.,

$$\sum_s \rightarrow \int ds. \quad (103)$$

As a result, (64), (65), and (80) take the form (after the integration over φ)

$$\frac{dW}{du} = \frac{m^2 e^2}{16\pi q_0 (1+u)^2} \int ds \eta_s F(s, u), \quad (104)$$

where

$$F \equiv -2J_s^2(z) \left(2 + \frac{u-3}{2(u+1)} \frac{s^2 m_{ph}^2}{m^2} \right) + 4\xi^2 \left[\left(\frac{s^2}{z^2} - 1 \right) J_s^2(z) + J_s'^2(z) \right]. \quad (105)$$

In addition, the relation between a Bessel function with a large index ($s \gg 1$) to the Airy function [70] is employed

$$J_s(z) \approx \left(\frac{2}{s} \right)^{1/3} \text{Ai}(y), \quad (106)$$

where $\text{Ai}(y) \equiv (1/\pi) \int_0^\infty dt \cos(t^3/3 + yt)$ and

$$y \equiv \left(\frac{s}{2} \right)^{2/3} \left(1 - \frac{z^2}{s^2} \right). \quad (107)$$

Let us write down the expressions appearing in (105) in terms of y ,

$$\left(\frac{s^2}{z^2} - 1 \right) J_s^2(z) = \left(\frac{2}{s} \right)^{4/3} \frac{y}{1 - (2/s)^{2/3} y} \text{Ai}^2(y) \quad (108)$$

and

$$J_s'^2(z) = \left(\frac{2}{s} \right)^{4/3} \text{Ai}'^2(y) \sqrt{1 - y \left(\frac{2}{s} \right)^{2/3}}. \quad (109)$$

Since the emission is attributed mainly to $z \rightarrow s$, we have $y \left(\frac{2}{s} \right)^{2/3} \ll 1$ and therefore the root in (109) and the denominator in (108) may be approximated by 1. Finally, we obtain

$$F \approx -4 \left(\frac{2}{s} \right)^{2/3} \text{Ai}^2(y) + 4 \left(\frac{2}{s} \right)^{4/3} \xi^2 [y \text{Ai}'^2(y) + \text{Ai}^2(y)]. \quad (110)$$

The continuum approximation is applicable if the harmonics overlap to create a continuous spectrum. In order to

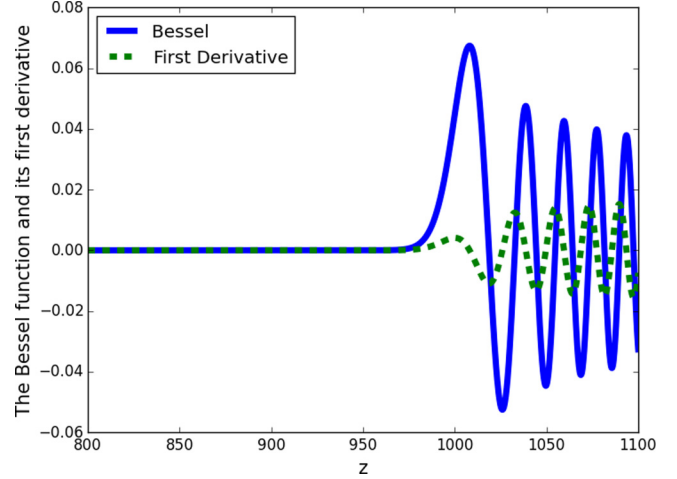


FIG. 1. Bessel function $J_s(z)$ and its derivative $J'_s(z)$ for $s = 1000$.

formulate the continuum condition, a better understanding of a single harmonic structure is required. The contribution of a single harmonic, as derived above, is a function of the corresponding Bessel function and its derivative $J_s(z), J'_s(z)$. The argument z is a function of u and one may prove that it lies in the range $0 < z < z_{\max}$. In the Volkov-Ritus case, the maximal value of z is

$$z_{\max}^V = s(1 - 1/2\xi^2), \quad (111)$$

as was derived in [44]. For the present solution, (91), (92), and (95) imply that z_{\max} is given by

$$z_{\max} = \frac{eap_{\text{out}}}{k \cdot q + sm_{ph}^2} \frac{\eta_s(\eta_s \kappa_s + 1)}{\sqrt{\eta_s^4 \kappa_s^2 - 1}}. \quad (112)$$

One may show analytically that it always falls behind z_{\max}^V .

An illustration of the Bessel function for large s appears in Fig. 1. As can be seen, the Bessel function and its derivative vanish through most of the range $0 < z < s$, but rise abruptly near $z = s$. Hence, the contribution to the emission comes from this region. Let us estimate the argument z_r for which the function starts rising. For this purpose, the relation between the Bessel function and the Airy function (106) is invoked once again. The Airy function is approximately zero if its argument satisfies $y_r > 3$. Accordingly, z_r obeys

$$y_r = 3 = \left(\frac{s}{2} \right)^{2/3} \left(1 - \frac{z_r^2}{s^2} \right). \quad (113)$$

For the Bessel function plotted above ($s = 1000$), this estimation yields $z_r = 976$, in agreement with Fig. 1. Since for large s we have $z_r \approx s$, a quantity measuring the distance between z_r and s is introduced

$$\epsilon_s^r \equiv \frac{s - z_r}{s}. \quad (114)$$

Substituting (114) into (113), ϵ_s^r is obtained

$$\epsilon_s^r = \frac{3}{2} \left(\frac{2}{s} \right)^{2/3}. \quad (115)$$

The deviation of z_{\max} with respect to s is denoted similarly by

$$\epsilon_s^{\max} \equiv \frac{s - z_{\max}}{s}. \quad (116)$$

Due to (111), the deviation of z_{\max}^V from s may be readily obtained

$$\epsilon_s^V \equiv \frac{s - z_{\max}^V}{s} = \frac{1}{2\xi^2}. \quad (117)$$

Having discussed the Bessel function behavior in the relevant regime, the width of a given harmonic may be readily obtained. The u values corresponding to the harmonic boundaries satisfy the equation $z(u) = z_r$. In terms of z_{\max} , the argument z given in (91) may be written as

$$z(u) = \frac{z_{\max}}{\bar{D}_s} \sqrt{\bar{A}_s u^2 + \bar{B}_s u + \bar{C}_s}. \quad (118)$$

Employing (118), the equation for the harmonic boundaries reads

$$\bar{A}_s u^2 + \bar{B}_s u + \bar{C}_s = \bar{D}_s^2 \left(\frac{1 - \epsilon_s^r}{1 - \epsilon_s^{\max}} \right)^2. \quad (119)$$

Notice that z_{\max}, z_r were replaced by $\epsilon_s^r, \epsilon_s^{\max}$ according to Eqs. (115) and (116). The difference Δu_s between the solutions $u_{s,2}, u_{s,1}$ of (119), corresponding the harmonic width, is

$$\Delta u_s = \frac{1}{\bar{A}_s} \sqrt{\bar{B}_s^2 - 4\bar{A}_s \left[\bar{C}_s - \bar{D}_s^2 \left(\frac{1 - \epsilon_s^r}{1 - \epsilon_s^{\max}} \right)^2 \right]}. \quad (120)$$

With the above expression at hand, the continuum condition may be quantitatively formulated. As mentioned before, the spectrum is continuous if the harmonics overlap. It occurs if the spacing between two neighboring harmonics is much smaller than the harmonic width, i.e.,

$$\frac{\Delta u_s}{u_{s+1}^m - u_s^m} \gg 1. \quad (121)$$

The inequality (121) is harmonic dependent. In order to use the continuum formula, (121) has to hold for all the harmonics with non-negligible contribution to the spectrum.

Now let us show how, for vanishing m_{ph} , the expressions derived above (104) and (110) recover the Volkov-Ritus continuum approximation. In the Volkov limit, the maximal value of the Bessel argument is (111), corresponding to $y = (u/2\chi)^{2/3}$. Expanding y in the vicinity of this point, (107) becomes (as was shown in [44])

$$y = \left(\frac{u}{2\chi} \right)^{2/3} [1 + \rho^2], \quad (122)$$

where the expansion parameter ρ is related to s by

$$\rho \equiv \xi \left(\frac{s\chi}{\xi^3 u} - 1 - \frac{1}{2x^2} \right). \quad (123)$$

The substitution of (110) and (123) in (104) yields the Volkov-Ritus continuum approximation

$$\frac{dW}{du} = \frac{e^2 m^2}{2\pi^3 q_0} \int d\rho \frac{(u/2\chi)^{1/3}}{(1+u)^2} \times \left\{ -\text{Ai}^2(y) + \left(\frac{2u}{\chi} \right)^{2/3} [y\text{Ai}^2(y) + \text{Ai}'^2(y)] \right\}. \quad (124)$$

The expression above coincides with the rate of a particle in a constant crossed field. It should be mentioned that in this case, since the field frequency is assumed to go to zero, one may replace q_0 with Π_0 (see [44]).

VIII. COHERENCE TIME INTERVAL

In this work a periodic electric field with an infinite duration is considered. In the following we discuss the realistic pulse duration required for the buildup of the spectral structure of the emitted radiation. In other words, we look for the effective time interval over which the radiation is formed. Our analysis closely follows the one presented by Ritus [44], with several necessary modifications. For the sake of the argument, let us perform the integration in (66) over the spatial coordinates only (in the laboratory framework):

$$iT = \int_{-\infty}^{\infty} dt M(t) e^{-i(q_0 - q'_0 - \omega')t} \delta^{(3)}(\mathbf{q} - \mathbf{q}' - \mathbf{k}'), \quad (125)$$

where

$$M(t) = (M_1 + M_2 \cos \omega t + M_3 \sin \omega t) e^{iz \sin(\omega t - \phi_0)} \quad (126)$$

is a periodic function whose cycle is $\tau = 2\pi/\omega$ and z is given by (91). The coefficients M_1, M_2, M_3 may be found in Sec. V and bear no importance for the present discussion. As explained in Sec. V, the evaluation of the integral yields an infinite sum of energy-momentum-conservation δ functions (77), each corresponding to a different number s of laser photons participating in the process. We consider a given harmonic s and seek the time interval over which it is formed. According to the corresponding δ function, we have $q_0 - q'_0 - \omega' = -s\omega$. As a result, (125) takes the form

$$iT = \int_{-\infty}^{\infty} dt M(t) e^{-is\omega t} \delta^{(3)}(\mathbf{q} - \mathbf{q}' - \mathbf{k}'). \quad (127)$$

The integral (127), if performed over a single cycle, yields the Fourier coefficient \mathcal{M}_s . The summation over an infinite number of cycles results in the δ function. Equation (127) implies that the contribution to the emitted radiation is periodic in time.

In the following we focus our attention on a single cycle. As derived in Sec. V, \mathcal{M}_s constitutes a combination of the Bessel function and its first derivative (77). The same result may be obtained by integration of (127) over a single cycle due to the identity

$$J_s(z) = \omega \int_{-\tau/2}^{\tau/2} dt e^{i(z \sin \omega t - s\omega t)}. \quad (128)$$

Owing to the rapidly oscillating exponent argument, the main contribution to the integral originates from a narrow interval Δt_c around $t = 0$ (where the argument vanishes). This interval

may be written [44] in terms of z, s as $\Delta t_c = \tau \cosh^{-1}(s/z)$. Approximating z by z_{\max} and using (116) one obtains $\Delta t_c = \tau \cosh^{-1}[1/(1 - \epsilon_s^{\max})]$. Since $\epsilon_s^{\max} < \epsilon_s^r$ and according to (115), we have $\epsilon_s^{\max} \ll 1$ and hence $\Delta t_c \ll \tau$ as long as $s \gg 1$. In the Volkov-Ritus case ϵ_s^v is given analytically by (117), leading to $\Delta t_c = \tau/\xi$ [44]. An analogous analysis regarding $J'_s(z)$ leads to the same result for Δt_c .

Let us discuss our findings. We have seen that the contribution to the emission is periodic in time. However, for $\xi \gg 1$, the emission of a given harmonic takes place over a narrow time interval Δt_c rather than the entire cycle. This interval, over which the radiation is formed, is termed the coherence time interval. Since the coherence time interval is much shorter than a single cycle ($\Delta t_c \ll \tau$), the emission process may be regarded as instantaneous. Namely, it does not depend on the temporal history of the EM field. However, this argument applies only in the continuum limit for the following reason. On account of the finite integration interval Δt_c , the energy-momentum-conservation δ function becomes a sinc function with a spectral width $\Delta\omega' \approx 1/\Delta t_c$. Since the coherence interval obtained above is much shorter than τ , we have $\Delta s \gg 1$, where $\Delta s = \Delta\omega'/\omega$ is the number of harmonics included in the interval $\Delta\omega'$. As a result, the approximated Fourier transform (125) of $M(t)$ in the vicinity of $\omega' = q_0 - q'_0 + s\omega$ consists also of contributions from Δs neighboring harmonics. Consequently, limiting the integration to the coherence interval yields satisfactory results for the spectrum only if it changes over an energy scale much greater than $\Delta\omega' = \omega\Delta s$. This requires the fulfillment of the following conditions. First, the harmonics should overlap, i.e., the continuous approximation should hold. Second, the uncertainty Δs should be smaller than the number of absorbed laser photons, i.e., $\Delta s \ll s$. In the Volkov case this relation is automatically satisfied since $\Delta s \approx \xi$ and $s \approx \xi^3$. In our case this condition should be verified numerically for the particular physical parameters under consideration.

As a consequence of the above discussion, the results obtained in this paper are valid even for a few-cycle pulse provided $\Delta s \ll s$ and the continuum approximation is valid. Beyond this regime, our analysis is adequate only for a long pulse containing tens of cycles at least.

IX. EMISSION SPECTRUM

In the previous sections, the rate W was calculated as a function of the invariant dimensionless variables u, φ . In practice, we are interested in the spectrum of the emitted power P as a function of the outgoing photon energy ω' . In the following, the transformation between these quantities is discussed. Since the numerical results appearing in this work were calculated for problems without a φ dependence (see the following section), it is omitted from this discussion as well. The emitted power spectrum is given by

$$\frac{dP}{d\omega'} = \sum_s \omega' \frac{dW_s}{d\omega'} = \sum_s \omega' \frac{dW_s}{du} \frac{du}{d\omega'}. \quad (129)$$

The relation between u and ω' stems from the definition (55),

$$u = \frac{\omega'}{E_s^{\text{lab}} - \omega'}, \quad (130)$$

where $E_s^{\text{lab}} = q_0^{\text{lab}} + s\omega = \omega' + q_0^{\text{lab}'}$ is the total energy in the laboratory frame. The derivative is given by

$$\frac{du}{d\omega'} = \frac{1}{E_s^{\text{lab}} - \omega'} + \frac{\omega'}{(E_s^{\text{lab}} - \omega')^2} = \frac{E_s^{\text{lab}}}{(E_s^{\text{lab}} - \omega')^2}, \quad (131)$$

where the derivative of E_s^{lab} with respect to ω' vanishes. If $q_0^{\text{lab}} \gg s\omega$ for all the harmonics with non-negligible contribution to the spectrum, which holds for our calculation, the energy E_s^{lab} is the same for all the harmonics. As a result, $\omega' \frac{du}{d\omega'}$ may be extracted from the summation over s ,

$$\frac{dP}{d\omega'} = \frac{\omega'}{(q_0^{\text{lab}} - \omega')^2} \frac{dW}{du}. \quad (132)$$

This is the final expression relating dW/du obtained earlier to the actual measurable spectrum $dP/d\omega'$.

To conclude the analytical part of the paper, let us summarize the final expressions obtained so far. The emission probability is given by (64) and (65), the matrix element is given by (80), and the variable z is calculated using (70), (89), and (90). In the continuum approximation, these expressions are replaced by (110), (104), (107), and (91). The relation between the emission probability and the spectrum in the laboratory frame was obtained in this section, Eq. (132).

X. NUMERICAL RESULTS

A. Optical laser

In the following the radiation emitted by an electron interacting with a rotating electric field (in the laboratory frame) is numerically investigated. The field vector potential is given by (26) and the wave vector is $k^{\text{lab}} = (m_{ph}, 0, 0, 0)$ (see Sec. III for details). It yields a homogenous electric field rotating in the x - y plane with frequency $\omega = m_{ph}$. As discussed in Sec. II, it approximates the field in the vicinity of the antinode of a standing wave created by counterpropagating beams. The electron initial asymptotic momentum takes the form $p^{\text{lab}} = (p_0, 0, 0, p_z)$ and the corresponding quasimomentum q is related to the asymptotic momentum by (29). The electron initial momentum was chosen to be perpendicular to the field plane in order to avoid dependence on φ [since $q \cdot a_1 = q \cdot a_2 = 0$; see Eq. (91)]. The laser photons energy is $\omega = m_{ph} = 1.6$ eV, corresponding to Ti:sapphire laser. The intensity was chosen to be the present-day record [26], $I = 10^{22}$ W/cm², leading to a normalized amplitude of $\xi = 50$.

In Figs. 2 and 4–7 the emitted photon spectrum is presented for several asymptotic momentum values. The solid line corresponds to our solution and was calculated by (64), (65), and (80). It should be mentioned that for the parameters of Figs. 2, 4, and 5 the continuum approximation (104), (110), and (91) is adequate and gives exactly the same spectrum as the full calculation. Our reference model (represented by the dashed line) is the Volkov-Ritus rate in the constant crossed field limit (124) and (102). As discussed in the Introduction, this model is commonly assumed to be adequate for an arbitrary field configuration given that (5) is satisfied, which holds in the cases under consideration. The evaluation of (124) requires three quantities: χ , ξ , and Π_0 . The quantity Π_0 is taken from (35) and χ is given in (36). Since the configuration considered

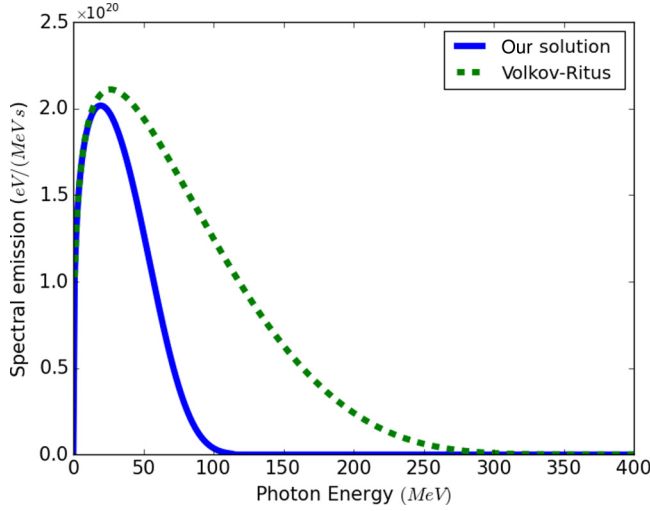


FIG. 2. Spectral emission according to our solution (solid curve) and the Volkov-Ritus rate (dashed curve) for $\xi = 50$, $\omega = 1.6$ eV, and $\mathbf{p}^{\text{lab}} = (0, 0, 1000 \text{ m})$.

here satisfies $A^{cl} \cdot p = 0$, the quantum parameter takes the simplified form

$$\chi = \frac{ea(k \cdot q)}{m^3}. \quad (133)$$

Notice that even though Π_μ is time dependent, χ is constant in time and changes only due to the emission process.

Figure 2 shows the emitted spectrum for $p_z^{\text{lab}} = 1000 \text{ m}$. Namely, the electron is accelerated towards the laser with an energy of 0.5 GeV. Such conditions may be achieved either by a standard accelerator (such as SLAC [71]) or by a laser-plasma accelerator [40]. Since this configuration parameters correspond to $\chi = 0.15$, it lies in the quantum regime. The two models coincide for soft outgoing photons ($< 30 \text{ MeV}$) but for higher energies the present model decreases much faster. Specifically, the spectrum corresponding to the present solution dies out at $\omega'_* \approx 100 \text{ MeV}$, while for the Volkov-Ritus case we have $\omega'^V_* \approx 300 \text{ MeV}$. The asterisk stands for the cutoff energy, meaning that the emission for $\omega' > \omega'_*$ is negligible (roughly speaking, less than 1% of the spectrum peak value). Moreover, the total emitted power is $P = 1.1 \times 10^{22} \text{ eV/s}$ and $P^V = 2.5 \times 10^{22} \text{ eV/s}$, respectively, namely, twice larger for the Volkov-Ritus calculation.

In order to account for the spectral difference exhibited in Fig. 2, we seek a theoretical estimation for the cutoff harmonic s_* . In Sec. VII we have seen that the Bessel function of a given index s goes to zero if its argument z satisfies $z < z_r = s(1 - \epsilon'_s)$. As a result, if the maximal argument of a given s , $z_{\text{max}} = s(1 - \epsilon_s^{\text{max}})$, is smaller than z_r , the contribution of this harmonic should be negligible. This insight enables us to write down the cutoff condition $\epsilon_s^{\text{max}} = \epsilon'_s$ satisfied by the cutoff harmonic s_* . Figure 3 shows the dependence of ϵ'_s , ϵ_s^{max} , and ϵ_s^V on the harmonic index s for the same physical parameters. According to the intersection points, one can deduce the cutoff harmonic: $s_* \approx 2.3 \times 10^5$ for our present model and $s_*^V \approx 1.3 \times 10^6$ for the Volkov-Ritus case.

Now let us calculate the energy ω'_* corresponding to this harmonic and compare it with the one inspected from the

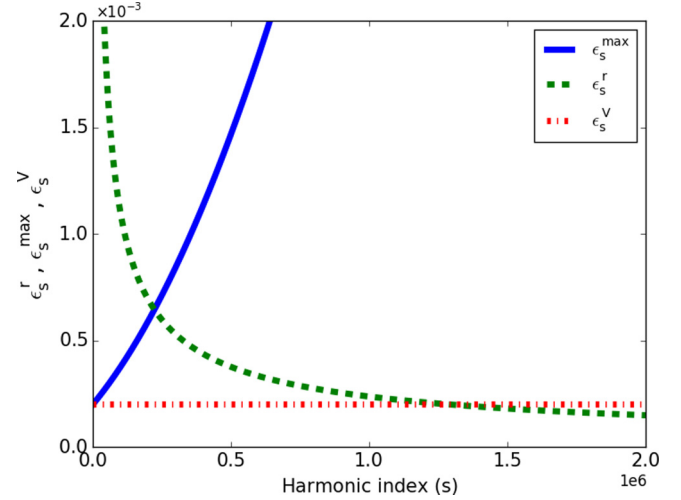


FIG. 3. Dimensionless quantities ϵ_s^{max} , ϵ'_s , and ϵ_s^V as a function of the harmonic index s . The solid line stands for ϵ_s^{max} , representing the normalized deviation of the Bessel argument z_{max} from s and given in (116). The dashed line stands for ϵ'_s , representing the normalized deviation of the Bessel argument z_r from s and given in (115). The dot-dashed line stands for ϵ_s^V , representing the normalized deviation of the Bessel argument z_{max}^V from s and given in (117).

numerical spectrum exhibited in Fig. 2. For this purpose, several quantities have to be evaluated: $E_{s_*} = 62.3 \text{ m}$, $\kappa_{s_*} = 4.6$, and $\eta_{s_*} = 1.001$, where Eqs. (48), (57), and (60) were used. It allows us to calculate the u value for which this harmonic contributes (94), namely, $u_{s_*}^m \approx 0.27$. Plugging it into (131), one finds that the spectrum should die out at $\omega'_* \approx 110 \text{ MeV}$. An analogous procedure for the Volkov-Ritus model yields $\kappa_{s_*} = 1.67$, $u_{s_*}^m = 1.5$, and thus $\omega'^V_* \approx 305 \text{ MeV}$. Both estimations are in excellent agreement with the numerical calculation of Fig. 2.

According to the numerical calculation, this effect (i.e., a lower cutoff for the present model spectrum) decreases for increasing asymptotic momentum. The spectra of the two models coincide for $p_z > 1.5 \times 10^4 \text{ m}$. In the following the opposite limit is explored; the asymptotic momentum is gradually reduced to nonrelativistic values.

In Fig. 4 the momentum is equal to the field amplitude, i.e., $p_z^{\text{lab}} = 50 \text{ m}$. This case is of special interest as it is the maximal momentum possible if the particle is accelerated by the field itself (without using an external accelerator). The difference between the models is analogous to the one appearing in Fig. 2 but more pronounced: Now the total emitted power is $P = 0.15 \times 10^{20} \text{ eV/s}$ and $P^V = 2.3 \times 10^{20} \text{ eV/s}$ and the cutoff is $\omega'_* = 200 \text{ keV}$ and $\omega'^V_* = 4000 \text{ keV}$, respectively. Notice that due to the lower asymptotic momentum, the spectral cutoff and the emitted power of both models are reduced orders of magnitude compared to those in Fig. 2.

In Fig. 5 the incoming momentum is an order of magnitude smaller than the field amplitude ($p_z^{\text{lab}} = 5 \text{ m}$). The total emitted power is $P = 0.06 \times 10^{20} \text{ eV/s}$ and $P^V = 1.17 \times 10^{20} \text{ eV/s}$ and the cutoff is $\omega'_* = 75 \text{ keV}$ and $\omega'^V_* = 2000 \text{ keV}$, respectively. That is to say, the emitted power corresponding to the present solution is lower by a factor of 20 than the power predicted by the Volkov-Ritus model. It can be seen that as

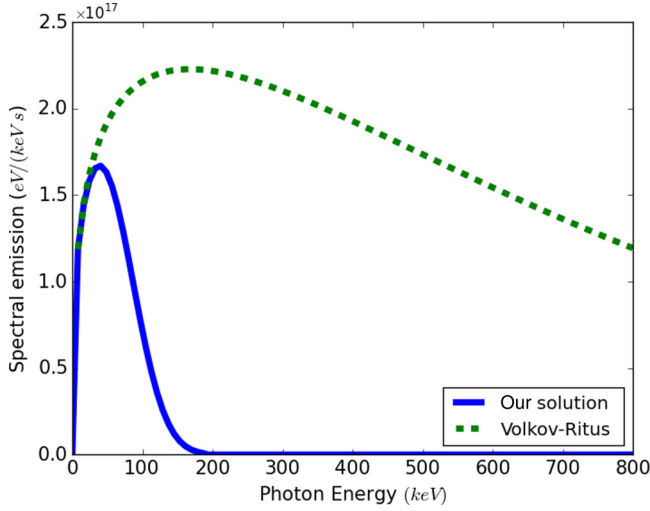


FIG. 4. Spectral emission according to our solution (solid curve) and the Volkov-Ritus rate (dashed curve) for $\xi = 50$, $\omega = 1.6$ eV, and $\mathbf{p}^{\text{lab}} = (0,0,50$ m).

compared to Fig. 4, the spectral shape and the maximum value of $dP/d\omega'$ remain the same for both models. The difference is in the lower cutoff and, as a result, the total emitted power. The reason lies in the lower value of $k \cdot q$ and therefore of χ .

In Fig. 6 the incoming momentum is decreased even lower ($p_z^{\text{lab}} = 0.01$ m), giving rise to an interesting phenomenon. The harmonics width becomes smaller than the spacing between following harmonics and consequently the spectrum is no longer continuous but takes a comblike structure. It corresponds to the breakdown of the continuum condition derived in Eq. (121).

In the following we suggest two qualitative explanations for this phenomenon. The classical one is that for negligible p_z values, the electron motion follows the vector potential, as can be inferred from (35). Consequently, the motion is circular. In this case, as was found long ago by Schott, the particle radiates

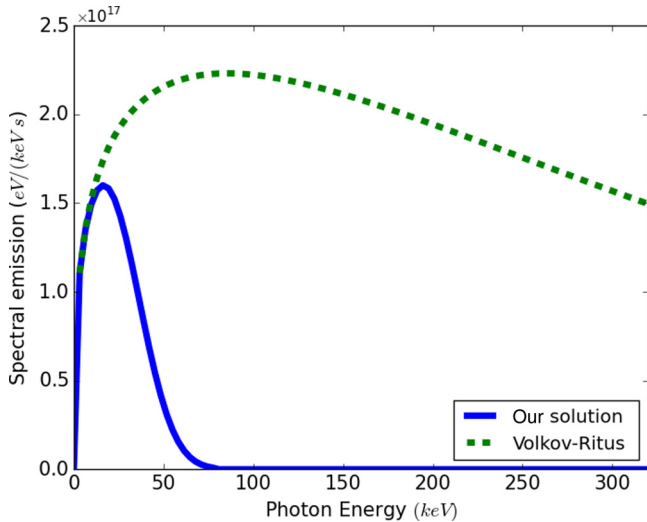


FIG. 5. Spectral emission according to our solution (solid curve) and the Volkov-Ritus rate (dashed curve) for $\xi = 50$, $\omega = 1.6$ eV, and $\mathbf{p}^{\text{lab}} = (0,0,5$ m).

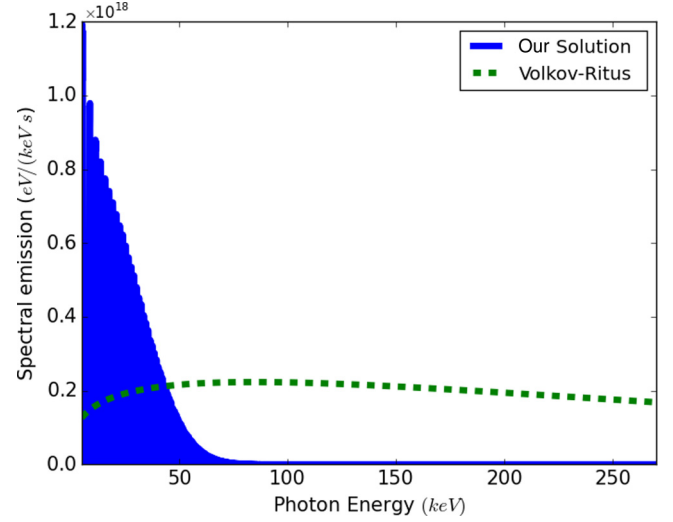


FIG. 6. Spectral emission according to our solution (solid curve) and the Volkov-Ritus rate (dashed curve) for $\xi = 50$, $\omega = 1.6$ eV, and $\mathbf{p}^{\text{lab}} = (0,0,0.01$ m).

discrete harmonics [72,73]. It may also be readily seen from the energy-momentum conservation (43). In the classical case $q \cdot q \approx q \cdot q'$. Therefore,

$$sq \cdot k = q \cdot k'. \quad (134)$$

Writing the above equation in the laboratory frame, one obtains

$$\omega' = \frac{s\omega q_0^{\text{lab}}}{q_0^{\text{lab}} - |\mathbf{q}|^{\text{lab}} \cos \gamma} \approx s\omega, \quad (135)$$

where γ is the angle between \mathbf{q}' and \mathbf{k}' in the laboratory frame. Since the second term in the denominator is negligible with respect to the first, the emitted harmonics are simply multiplication of the original one.

From the quantum point of view, we have seen in Sec. IV that in the center-of-mass frame the angle of the outgoing photon may get any value, but its energy has a certain value k'_0 . Transforming to the laboratory frame of reference, different emission angles correspond to different Lorentz transformations, giving rise to an energy spread. As a result, the closer the laboratory frame is to the center-of-mass frame of a given harmonic, the narrower its width is. This condition is achieved by lowering the incoming momentum p_z .

Figures 7 and 8 are zoomed-in presentations of Fig. 6 in different spectral regions. Figure 7 shows a range of 8 eV in the soft part of the spectrum and Fig. 8 shows the same range near the peak. They demonstrate that the harmonics width is extremely small for low-energy photons and increases with the photon energy, in accord with the explanation above.

B. X-ray laser

In this section another possible experimental setup is discussed. The optical laser is replaced by an x-ray laser with the parameters of the LCLS x-ray free-electron laser facility [31], i.e., $I = 4 \times 10^{20}$ W/cm² and $\omega = m_{ph} = 10$ keV corresponding to $\xi = 2 \times 10^{-3}$. Due to the small value of ξ , the emission involve only the two first harmonics and the continuum approximation could not be used. As a result, the

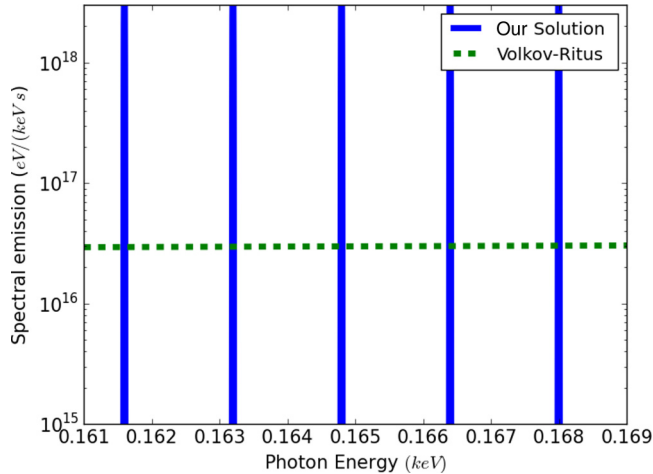


FIG. 7. Zoom in of Fig. 6 in the range 161–169 eV.

constant crossed field condition (5) is not satisfied and the Volkov-Ritus model is inapplicable in a rotating electric field even according to the Nikishov-Ritus assumption described in the Introduction. Nevertheless, in the absence of any other adequate model, it is used as a reference for our prediction. Consequently, the Volkov-Ritus rate was calculated by employing the full expression (104), (96), and (102) instead of the continuum expression used for the optical laser above.

Figure 9 compares the emission predicted by the present solution to the Volkov-Ritus one for nonrelativistic asymptotic momentum $p_z^{\text{lab}} = 10^{-4}$ m. According to (59), (57), and (94), the first and second harmonics correspond to $u_s^m = 0.01, 0.02$, respectively. Hence, the scattering is in the weakly quantum regime [see the discussion below Eq. (55)]. The energy contained under the curves is roughly identical, as opposed to the optical laser calculations above. The difference in this case lies in the width of the harmonics. The mechanism behind the narrowing is the same as that encountered in Figs. 6–8. The second harmonic is of special interest for several reasons. First, the width differences are more pronounced for this harmonic. Second, it stems from the nonlinearity of the

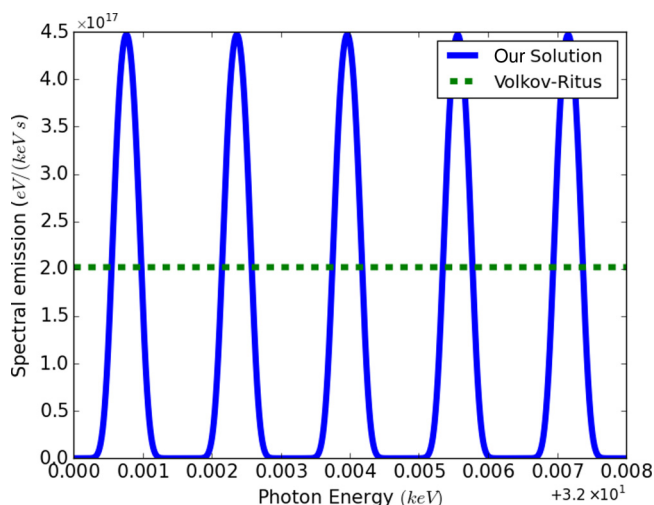
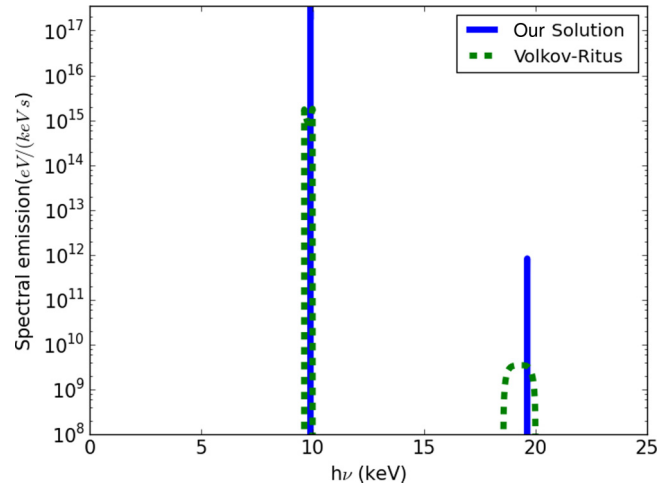


FIG. 8. Zoom in of Fig. 6 in the range 32–32.008 keV.


 FIG. 9. Spectral emission according to our solution (solid curve) and the Volkov-Ritus rate (dashed curve) for $\xi = 2 \times 10^{-3}$, $\omega = 10$ keV, and $\mathbf{p}^{\text{lab}} = (0, 0, 10^{-4})$ m.

interaction and could be seen for strong fields only. Third, a measurement of the second harmonic under similar conditions was recently demonstrated [74]. It should be stressed that our result could not be compared with this specific experiment since it was not carried out in a standing wave. However, it shows that an experimental test of our calculation is possible with present-day facilities. The advantage of this experimental setup over the former one (the optical laser) is that the quantum regime can be achieved without an external accelerator.

XI. CONCLUSION

In this article the nonlinear Compton scattering rate in a rotating field was investigated. For the sake of this purpose, we employed an analytical solution to the Klein-Gordon equation describing a particle in the presence of this field configuration, recently derived by the present authors [58]. A closed analytical expression for the relevant matrix element was obtained in Eq. (80).

Furthermore, we have shown that for strong fields ($\xi \gg 1$) and initial asymptotic momentum satisfying the condition (121), the spectrum may be approximated by a continuous function instead of discrete harmonics sum. This is a generalization of the familiar continuum approximation of the Volkov-Ritus rate [2]. The final expression (104) and (110) is easy to calculate and may be employed in kinetic laser-plasma calculations.

Numerical calculations of the emitted photon spectrum according to the present rate were carried out and compared with the Volkov-Ritus rate. Physical parameters corresponding to the state-of-the-art facilities of both optical lasers ($I = 10^{22}$ W/cm² and $\omega = 1.6$ eV) and XFEL lasers ($I = 4 \times 10^{20}$ W/cm² and $\omega = 10$ keV) were chosen.

In the first case (optical laser), the Volkov-Ritus rate reduces to the constant crossed field rate, frequently used in QED PIC simulations. The following points arise from the comparison.

(i) The deviation between our expression and the Volkov-Ritus one in the total emitted power grows for decreasing incoming particle asymptotic momentum p_z^{lab} and amounts

to a factor of 20. In addition, the spectrum cutoff energy is considerably lower for our present solution. As an explanation for this phenomenon, a semianalytical way to determine the cutoff energy was suggested and achieved good agreement with the calculated spectrum. The discrepancy between our model and the Ritus-Volkov one decreases for increasing p_z^{lab} . The value above which both models coincide was found by numerical means.

(ii) For $p_z^{\text{lab}} \ll ea$ the energetic width of the harmonics that compose the spectrum falls beneath the spacing between them. As a result, the spectrum structure becomes comblike, as opposed to the continuous shape of the Volkov-Ritus rate under these conditions. An intuitive explanation for the discrepancy was suggested. This phenomenon is clear evidence of the imprint of the rotating frequency on the emission spectrum, as opposed to the constant field paradigm.

In the second case (x-ray laser), the emitted power according to the models under consideration was approximately equivalent. However, the present solution predicted much narrower harmonics. The mechanism behind this narrowing is the same as for the optical laser. The importance of the x-ray laser setup stems from the fact that it does not require high asymptotic momentum. As a result, it enables experimental verification of our model in the quantum regime without using an accelerator (as opposed to the optical laser setup).

To conclude, the above calculations may be experimentally tested for present-day laser systems. In addition, they may be of great importance in the context of PIC QED calculations of the QED cascade mechanism assumed to be measurable for the next-generation laser facilities.

APPENDIX A

In the following the relation (56) between u and $\cos \theta$ is explicitly derived. Substituting k' from the energy-momentum conservation (43) into the definition of u (55), we arrive at

$$u = \frac{sm_{ph}^2 + k \cdot q}{k \cdot q'} - 1. \quad (\text{A1})$$

Let us write down the explicit expression for u in the center-of-mass frame. Using (44) and (45), the numerator reads

$$k \cdot q + sm_{ph}^2 = k_0 q_0 + p_{\text{in}}^2/s + sm_{ph}^2. \quad (\text{A2})$$

Since $k_0^2 = (p_{\text{in}}/s)^2 + m_{ph}^2$, the former equation becomes

$$k \cdot q + sm_{ph}^2 = k_0 q_0 + sk_0^2. \quad (\text{A3})$$

Employing the relation $E_s = sk_0 + q_0$, we find

$$k \cdot q + sm_{ph}^2 = k_0 E_s. \quad (\text{A4})$$

We substitute (A4) into (A1) and evaluate $k \cdot q'$ using (46).

$$u = \frac{sk_0 E_s}{sk_0 q'_0 - p_{\text{in}} p_{\text{out}} \cos \theta} - 1. \quad (\text{A5})$$

In terms of η_s [defined in (58)] it becomes

$$u = \frac{\eta_s E_s}{\eta_s q'_0 - p_{\text{out}} \cos \theta} - 1. \quad (\text{A6})$$

Hence, $\cos \theta$ can be obtained in terms of u ,

$$\cos \theta = \frac{\eta_s}{p_{\text{out}}} \left(q'_0 - \frac{E_s}{1+u} \right). \quad (\text{A7})$$

Substituting the expression (52) for p_{out} and using the identity

$$q'_0 = \sqrt{p_{\text{out}}^2 + m_*^2} = \frac{E_s^2 + m_*^2}{2E_s}, \quad (\text{A8})$$

we find

$$\cos \theta = \eta_s \left(\kappa_s - \frac{\kappa_s + 1}{1+u} \right), \quad (\text{A9})$$

where κ_s was defined in (57).

APPENDIX B

This Appendix is dedicated to the derivation of the matrix element expression (80). Substituting (77) into (79), we have

$$\begin{aligned} & \frac{1}{2} \sum_{\epsilon'} |\mathcal{M}|^2 \\ &= -2e^2 B^2 (m_*^2 + q \cdot q') + 2Bk \cdot (q + q') \\ & \quad \times [\bar{\alpha}_1 \text{Re}(B_1) + \bar{\alpha}_2 \text{Re}(B_2)] - 4eB(q + q') \\ & \quad \times [a_1 \text{Re}(B_1) + a_2 \text{Re}(B_2)] \\ & \quad - 4e^4 a^2 (|B_1|^2 + |B_2|^2) + e[\bar{\alpha}_1 B_1 + \bar{\alpha}_2 B_2]^2 m_{ph}^2, \end{aligned} \quad (\text{B1})$$

where Re denotes real part and the following definition is used:

$$\bar{\alpha}_i \equiv \frac{e(a_i \cdot q)}{(k \cdot q)} + \frac{e(a_i \cdot q')}{(k \cdot q')}, \quad i = 1, 2. \quad (\text{B2})$$

It should be mentioned that since $\mathcal{M}_\mu \propto e^{is\phi_0}$, this constant exponent does not contribute to \mathcal{M}^2 and thus may be omitted. As a result, B is real (while B_1, B_2 remain complex).

Before starting, let us examine the last term in Eq. (B1). It is of the same order of magnitude as the quantity δ assumed to be small in the present wave-function derivation (see Sec. III) and thus may be neglected. In order to simplify (B1), the term $k \cdot (q + q') \bar{\alpha}_1$ is further worked out

$$\begin{aligned} k \cdot (q + q') \bar{\alpha}_1 &= e(a_1 \cdot q) + e(a_1 \cdot q') \\ & \quad + e(a_1 \cdot q) \frac{k \cdot q'}{k \cdot q} + e(a_1 \cdot q') \frac{k \cdot q}{k \cdot q'}, \end{aligned} \quad (\text{B3})$$

where the explicit formula (B2) for $\bar{\alpha}_1$ was used. Due to the algebraic identities

$$\frac{k \cdot q}{k \cdot q'} = 1 + \frac{k \cdot (q - q')}{k \cdot q'}, \quad (\text{B4})$$

$$\frac{k \cdot q'}{k \cdot q} = 1 - \frac{k \cdot (q - q')}{k \cdot q}, \quad (\text{B5})$$

Eq. (B3) becomes

$$k \cdot (q + q') \bar{\alpha}_1 = 2e(a_1 \cdot q) + 2e(a_1 \cdot q') - \alpha_1 (q - q'), \quad (\text{B6})$$

where α_1 was defined in Eq. (68). Analogously, we have

$$k \cdot (q + q') \bar{\alpha}_2 = 2e(a_2 \cdot q) + 2e(a_2 \cdot q') - \alpha_2 (q - q'). \quad (\text{B7})$$

Substituting (B6) and (B7) into (B1), several terms cancel out and we are left with

$$\frac{1}{2} \sum_{\epsilon'} |\mathcal{M}|^2 = -2e^2 B^2 (m_*^2 + q \cdot q') - 4e^4 a^2 (|B_1|^2 + |B_2|^2) + 2eB(q - q') [\text{Re}(B_1)\alpha_1 + \text{Re}(B_2)\alpha_2]. \quad (\text{B8})$$

By virtue of the identity [44]

$$\alpha_1 B_1 + \alpha_2 B_2 = sB, \quad (\text{B9})$$

we obtain

$$\frac{1}{2} \sum_{\epsilon'} |\mathcal{M}|^2 = -2e^2 B^2 (m_*^2 + q \cdot q') - 4e^4 a^2 (|B_1|^2 + |B_2|^2) + 2e^2 s B^2 k \cdot (q - q'). \quad (\text{B10})$$

Employing (83) we have

$$k \cdot (q - q') = \frac{uk \cdot q + sm_{ph}^2}{u + 1}. \quad (\text{B11})$$

As a result, the matrix element becomes

$$\frac{1}{2} \sum_{\epsilon'} |\mathcal{M}|^2 = -2e^2 B^2 (m_*^2 + q \cdot q') - 4e^4 a^2 (|B_1|^2 + |B_2|^2) + 2e^2 s B^2 \frac{uk \cdot q + sm_{ph}^2}{u + 1}. \quad (\text{B12})$$

In order to proceed, let us express $q \cdot q'$ in terms of u . Multiplying (43) by q' , we obtain

$$q \cdot q' = m_*^2 + k' \cdot q' - sk' \cdot q'. \quad (\text{B13})$$

The center-of-mass energy may be written in terms of the outgoing 4-momenta

$$E_s^2 = (k' + q')^2 = m_*^2 + 2k' \cdot q'. \quad (\text{B14})$$

Therefore, $k' \cdot q'$ reads

$$k' \cdot q' = \frac{E_s^2 - m_*^2}{2}. \quad (\text{B15})$$

The substitution of (B15, 83) into (B13) yields

$$q \cdot q' = \frac{E_s^2 + m_*^2}{2} - \frac{s^2 m_{ph}^2 + s(k \cdot q)}{u + 1}. \quad (\text{B16})$$

With the aid of (B16), we get

$$\frac{1}{2} \sum_{\epsilon'} |\mathcal{M}|^2 = -2e^2 B^2 \left(2m_*^2 + \frac{u-3}{2(u+1)} s^2 m_{ph}^2 \right) - 4e^4 a^2 (|B_1|^2 + |B_2|^2). \quad (\text{B17})$$

Plugging B, B_1, B_2 , defined in (73)–(75), into (B17), we obtain the final expression

$$\frac{1}{2} \sum_{\epsilon'} |\mathcal{M}_{s,\epsilon'}|^2 = -2e^2 J_s^2(z) \left(2m_*^2 + \frac{u-3}{2(u+1)} s^2 m_{ph}^2 \right) + 4e^4 a^2 \left(\frac{s^2}{z^2} J_s^2(z) + J_s'^2(z) \right). \quad (\text{B18})$$

APPENDIX C

In this Appendix an expression for the component a_1 of the vector potential [defined in (21)] in the center-of-mass frame is obtained. The most general expression is

$$a_1 = a(R_0, R_1, 0, R_3). \quad (\text{C1})$$

For the moment, R_0, R_1, R_3 are unknown. Fortunately, a_1 is known to obey several identities and thus relations between these coefficients may be deduced. Since $a_1 \cdot k = 0$ we have

$$R_3 = R_0 \frac{\omega}{k_z} = R_0 \eta_s. \quad (\text{C2})$$

Due to $a_1 \cdot a_1 = -a^2$ we have

$$R_1 = \sqrt{1 - R_0^2 (\eta_s^2 - 1)}. \quad (\text{C3})$$

Hence, (C1) takes the form

$$a_1 = a [R_0, \sqrt{1 - R_0^2 (\eta_s^2 - 1)}, 0, R_0 \eta_s]. \quad (\text{C4})$$

The final step is to obtain R_0 in terms of the known quantity $q \cdot a_1$. For this purpose, we write $q \cdot a_1$ in the center-of-mass frame

$$q \cdot a_1 = a R_0 (q_0 + s\omega) = a R_0 E_s. \quad (\text{C5})$$

Therefore,

$$R_0 = \frac{q \cdot a_1}{a E_s}. \quad (\text{C6})$$

[1] L. V. Keldysh, *Sov. Phys. JETP* **20**, 1307 (1965).
 [2] A. I. Nikishov and V. I. Ritus, *Sov. Phys. JETP* **19**, 529 (1964).
 [3] W. H. Furry, *Phys. Rev.* **81**, 115 (1951).
 [4] D. M. Volkov, *Z. Phys.* **94**, 250 (1935).
 [5] V. B. Berestetskii, E. M. Lifshitz, and L. P. Pitaevskii, *Quantum Electrodynamics*, Course in Theoretical Physics Vol. 4 (Pergamon, Oxford, 1982).
 [6] I. I. Goldman, *Sov. Phys. JETP* **19**, 954 (1964).
 [7] L. S. Brown and T. W. B. Kibble, *Phys. Rev.* **133**, A705 (1964).
 [8] R. A. Neville and F. Rohrlich, *Phys. Rev. D* **3**, 1692 (1971).
 [9] J. H. Eberly, in *Progress in Optics*, edited by E. Wolf (North-Holland, Amsterdam, 1969), Vol. 7, p. 359.
 [10] F. B. Bunkin, A. E. Kazakov, and M. V. Fedorov, *Sov. Phys. Usp.* **15**, 416 (1973).

[11] N. B. Narozhny, A. R. Nikishov, and V. I. Ritus, *Sov. Phys. JETP* **20**, 622 (1965).
 [12] T. O. Müller and C. Müller, *Phys. Rev. A* **86**, 022109 (2012).
 [13] A. Di Piazza, E. Lötstedt, A. I. Milstein, and C. H. Keitel, *Phys. Rev. A* **81**, 062122 (2010).
 [14] P. Panek, J. Z. Kamiński, and F. Ehlötzky, *Phys. Rev. A* **65**, 022712 (2002).
 [15] P. Panek, J. Z. Kamiński, and F. Ehlötzky, *Phys. Rev. A* **69**, 013404 (2004).
 [16] E. Lötstedt and U. D. Jentschura, *Phys. Rev. A* **80**, 053419 (2009).
 [17] F. Mackenroth and A. Di Piazza, *Phys. Rev. A* **83**, 032106 (2011).

- [18] T. Heinzl, D. Seipt, and B. Kampfer, *Phys. Rev. A* **81**, 022125 (2010).
- [19] A. Ilderton, *Phys. Rev. Lett.* **106**, 020404 (2011).
- [20] M. Boca and V. Florescu, *Phys. Rev. A* **80**, 053403 (2009).
- [21] A. I. Titov, B. Kampfer, A. Hosaka, and H. Takabe, *Phys. Part. Nuclei* **47**, 456 (2016).
- [22] I. Berson, *Sov. Phys. JETP* **29**, 871 (1969).
- [23] I. Berson and J. Valdmanis, *J. Math. Phys.* **14**, 1481 (1973).
- [24] J. Bergou and S. Varro, *J. Phys. A* **14**, 2281 (1981).
- [25] D. Strickland and G. Mourou, *Opt. Commun.* **55**, 447 (1985).
- [26] V. Yanovsky, V. Chvykov, G. Kalinchenko, P. Rousseau, T. Planchon, T. Matsuoka, A. Maximchuk, J. Nees, G. Cheriaux, G. Mourou, and K. Krushelnik, *Opt. Express* **16**, 2109 (2008).
- [27] The ELI project homepage is <http://www.extreme-light-infrastructure.eu/>.
- [28] The XCELS project homepage is <http://www.xcels.iapras.ru>.
- [29] The HiPER project homepage is <http://www.hiper-laser.org/>.
- [30] The GEKKO EXA project homepage is in Japanese. The laser concept may be found at http://www.stfc.ac.uk/clf/resources/pdf/talk_3.pdf.
- [31] The Linac Coherent Light Source homepage is <https://lcls.slac.stanford.edu/>.
- [32] The SACLA homepage is <http://xfel.riken.jp/eng/index.html>.
- [33] The FLASH homepage is <http://flash.desy.de/>.
- [34] The XFEL homepage is <http://www.xfel.eu/>.
- [35] T. Tajima and G. Mourou, *Phys. Rev. ST Accel. Beams* **5**, 031301 (2002).
- [36] J. T. Mendonça and S. Eliezer, in *Applications of Laser-Plasma Interaction*, edited by S. Eliezer and K. Mima (CRC, Boca Raton, 2009).
- [37] F. Krausz and M. Ivanov, *Rev. Mod. Phys.* **81**, 163 (2009).
- [38] B. Dromey *et al.*, *Nat. Phys.* **2**, 456 (2006).
- [39] S. V. Bulanov, T. Z. Esirkepov, M. Kando, A. S. Pirozhkov, and N. N. Rosanov, *Phys. Usp.* **56**, 429 (2013).
- [40] E. Esarey, C. B. Schroeder, and W. P. Leemans, *Rev. Mod. Phys.* **81**, 1229 (2009).
- [41] A. Macchi, M. Borghesi, and M. Passoni, *Rev. Mod. Phys.* **85**, 751 (2013).
- [42] P. Chen, *Eur. Phys. J. Spec. Top.* **223**, 1121 (2014).
- [43] A. Di Piazza, C. Müller, K. Z. Hatsagortsyan, and C. H. Kietel, *Rev. Mod. Phys.* **84**, 1177 (2012).
- [44] V. I. Ritus, *J. Sov. Laser Res.* **6**, 497 (1985).
- [45] J. Schwinger, *Phys. Rev.* **82**, 664 (1951).
- [46] N. V. Zamfir, *Eur. Phys. J. Spec. Top.* **223**, 1221 (2014).
- [47] I. V. Sokolov, N. M. Naumova, J. A. Nees, and G. A. Mourou, *Phys. Rev. Lett.* **105**, 195005 (2010).
- [48] E. P. Liang, S. C. Wilks, and M. Tabak, *Phys. Rev. Lett.* **81**, 4887 (1998).
- [49] E. N. Nerush, I. Y. Kostyukov, A. M. Fedotov, N. B. Narozhny, N. V. Elkina, and H. Ruhl, *Phys. Rev. Lett.* **106**, 035001 (2011).
- [50] A. M. Fedotov, N. B. Narozhny, G. Mourou, and G. Korn, *Phys. Rev. Lett.* **105**, 080402 (2010).
- [51] N. V. Elkina, A. M. Fedotov, I. Y. Kostyukov, M. V. Legkov, N. B. Narozhny, E. N. Nerush, and H. Ruhl, *Phys. Rev. ST Accel. Beams* **14**, 054401 (2011).
- [52] I. V. Sokolov, M. N. Naumova, and J. A. Nees, *Phys. Plasmas* **18**, 093109 (2011).
- [53] C. P. Ridgers, C. S. Brady, R. Duclous, J. G. Kirk, K. Bennett, T. D. Arber, and A. R. Bell, *Phys. Plasmas* **20**, 056701 (2013).
- [54] C. P. Ridgers, C. S. Brady, R. Duclous, J. G. Kirk, K. Bennett, T. D. Arber, A. P. L. Robinson, and A. R. Bell, *Phys. Rev. Lett.* **108**, 165006 (2012).
- [55] C. S. Brady, C. P. Ridgers, T. D. Arber, A. R. Bell, and J. G. Kirk, *Phys. Rev. Lett.* **109**, 245006 (2012).
- [56] L. L. Ji, A. Pukhov, E. N. Nerush, I. Y. Kostyukov, B. F. Shen, and K. U. Akli, *Phys. Plasmas* **21**, 023109 (2014).
- [57] E. N. Nerush, V. F. Bashmakov, and I. Y. Kostyukov, *Phys. Plasmas* **18**, 083107 (2011).
- [58] E. Raicher, S. Eliezer, and A. Zigler, *Phys. Lett. B* **750**, 76 (2015).
- [59] F. Ehlötzky, K. Krajewska, and J. Z. Kaminski, *Rep. Prog. Phys.* **72**, 046401 (2009).
- [60] E. Raicher, S. Eliezer, and A. Zigler, *Phys. Plasmas* **21**, 053103 (2014).
- [61] S. Varro, *Laser Phys. Lett.* **10**, 095301 (2013).
- [62] S. Varro, *Laser Phys. Lett.* **11**, 016001 (2014).
- [63] F. S. Felber and J. H. Marburger, *J. Math. Phys.* **16**, 2089 (1975).
- [64] J. T. Mendonca and A. Serbeto, *Phys. Rev. E* **83**, 026406 (2011).
- [65] W. Becker, *Physica A* **87**, 601 (1977).
- [66] C. Cronstrom and M. Noga, *Phys. Lett. A* **60**, 137 (1977).
- [67] H. Hu and J. Huang, *Phys. Rev. A* **92**, 062105 (2015).
- [68] T. Heinzl, A. Ilderton, and B. King, *Phys. Rev. D* **94**, 065039 (2016).
- [69] M. E. Peskin and D. V. Schroeder, *An Introduction to Quantum Field Theory* (Perseus Books, Reading, 1995).
- [70] G. N. Watson, *A Treatise on the Theory of Bessel Functions* (Cambridge University Press, Cambridge, 1966).
- [71] C. Bamber, S. J. Boege, T. Koffas, T. Kotseroglou, A. C. Melissinos, D. D. Meyerhofer, D. A. Reis, W. Ragg, C. Bula, K. T. McDonald, E. J. Prebys, D. L. Burke, R. C. Field, G. Horton-Smith, J. E. Spencer, D. Walz, S. C. Berridge, W. M. Bugg, K. Shmakov, and A. W. Weidemann, *Phys. Rev. D* **60**, 092004 (1999).
- [72] G. A. Schott, *Electromagnetic Radiation* (Cambridge University Press, Cambridge, 1912).
- [73] L. D. Landau and E. M. Lifshitz, *The Classical Theory of Fields* (Reed, Oxford, 1975).
- [74] M. Fuchs *et al.*, *Nat. Phys.* **11**, 964 (2015).